

# The NA62 RICH Detector

Giuseppina Anzivino

*Department of Physics, University of Perugia and INFN, via A. Pascoli, 06123 Perugia, Italy*

**Abstract.** The goal of the CERN NA62 experiment is to measure the ultra-rare (Branching Ratio, BR  $\sim 10^{-10}$ ) charged kaon decay  $K^+ \rightarrow \pi^+ \nu \bar{\nu}$  with an accuracy of 10%. The main background, the  $K^+ \rightarrow \mu^+ \nu$  decay (BR  $\sim 63\%$ ), must be suppressed by a rejection factor of  $4 \times 10^{-13}$ . This can be accomplished using a combination of several methods and detectors. The RICH detector will contribute to this task and will also provide the pion crossing time with a resolution of the order of 100 ps. The details of the RICH project as well as the results from two different test beams performed on a RICH prototype will be presented.

**Keywords:** PID, RICH, timing

**PACS:** 29.40.Ka, 13.20.Eb

## INTRODUCTION

The NA62 experiment [1] will be installed at CERN in the North Area on an extracted beam from the SPS accelerator. The experiment aims to measure the Branching Ratio (BR) of the ultra-rare  $K^+ \rightarrow \pi^+ \nu \bar{\nu}$  decay with high accuracy. The Standard Model (SM) prediction [2] is very accurate,  $BR = (0.85 \pm 0.07) \times 10^{-10}$ , due to the extreme cleanliness of the process. On the other hand, the only experimental result [3],  $BR = (1.73^{+1.15}_{-1.05}) \times 10^{-10}$  based on 7 events, is twice as large as, but still compatible with, the SM prediction within errors. A new measurement of the BR with higher precision will allow one to perform a stringent test of the SM and probe possible new degrees of freedom beyond the SM. Sizable deviations from the SM are predicted by several models [4,5].

NA62 will collect  $\sim 100$  events in two years of data taking and will reach an accuracy of 10%. The experimental strategy is based on (i) an accurate kinematic reconstruction to disentangle the signal, (ii) a precise timing to associate the daughter particle, the pion, with the parent kaon, (iii) a system of efficient vetoes to reject events with  $\gamma$ 's and  $\mu$ 's, and (iv) a particle identification system to identify kaons in the charged beam and to distinguish pions from muons in the final state. The R&D phase of the experiment, which was started in 2007, has been completed. The construction of the different detectors of the apparatus is at a well-advanced stage and data taking is foreseen to commence in 2012-2013.

The main background, the decay  $K^+ \rightarrow \mu^+ \nu$  (BR  $\sim 63\%$ ), must be suppressed by a rejection factor of  $4 \times 10^{-13}$ . This can be accomplished using a combination of kinematical cuts ( $8 \times 10^{-6}$ ) and the different power of penetration through matter of pions and muons ( $10^{-5}$ ). A further suppression factor of  $5 \times 10^{-3}$  will be provided by a

Ring Imaging Cherenkov (RICH) detector in a momentum range between 15 and 35 GeV/c. The RICH detector must also provide the pion crossing time with a resolution of the order of 100 ps in order to minimize wrong matching with the parent particle measured by an upstream detector.

In a RICH detector [6], the Cherenkov light emitted at an angle  $\theta_C$  by a charged particle of velocity  $\beta c$ , which is larger than the speed of light in the crossed medium, is imaged by means of a spherical mirror onto a ring on its focal plane. In the case of small index of refraction  $n$ , as is typical of gas radiators, the ring radius  $r$  is related to the Cherenkov angle by  $\theta_C = r/f$  where  $f$  is the focal length of the mirror.

The NA62 RICH [7] detector is a tube that is  $\sim 18$  m long and  $\sim 3$  m in diameter. It is filled with neon at atmospheric pressure and room temperature, and it is equipped with a segmented 17 m focal length mirror at the downstream end and about 2000 photomultipliers (PMs) at the upstream end. Figure 1 shows a schematic drawing of the detector.

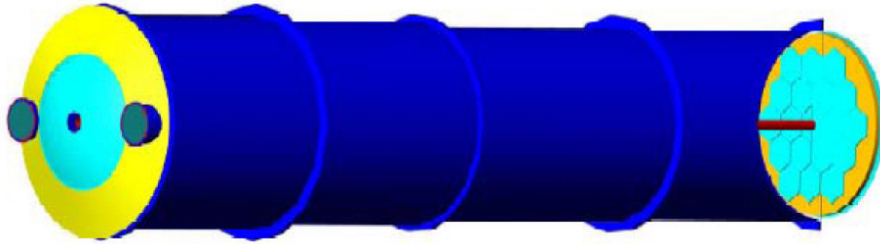


**FIGURE 1.** Schematic drawing of the RICH detector; the downstream section of the vessel is cut to show the mirrors and the beam pipe; the upstream section shows the PM assembly.

In order to achieve the required  $\pi$ - $\mu$  separation, the NA62 RICH detector must have a Cherenkov angle resolution better than  $80 \mu\text{rad}$ . Moreover, it must provide the crossing time of the pion produced in the  $K^+$  decay with a resolution of less than 100 ps, and it should give a fast signal for the first level trigger. The best  $\pi$ - $\mu$  separation is obtained when the lowest accepted momentum is close to the Cherenkov threshold. However, in order to have full efficiency for a 15 GeV/c momentum pion, the threshold should be about 20% smaller, i.e. 12.5 GeV/c; this value of the threshold corresponds to  $(n-1) = 62 \times 10^{-6}$ , which matches almost exactly the index of refraction of neon at atmospheric pressure; neon also guarantees a small dispersion. The smallness of  $(n-1)$  implies a low emission of Cherenkov photons per unit length that should be compensated with a long radiator. The NA62 RICH detector will make use of the maximum space available along the beam line: a vacuum resistant, structural steel cylindrical vessel is being fabricated; it is 18 m long and made of 4 longitudinal sections with decreasing diameter (4 to 3.4 m) with the beam pipe passing through. The total volume of about  $200 \text{ m}^3$  will be filled with neon gas in slight overpressure with respect to the external atmosphere; the total radiation length corresponds to  $5.6\% X_0$ . The non-reflectivity and the cleanliness of its inner surface will be ensured by a mat epoxy coating. After a vacuum cleaning procedure, neon will be inserted and kept for long data taking periods. No gas recirculation and purification system is foreseen. In case of opening of the vessel, the entire volume of gas will be replaced. The gas density stability will be below 1%, and gas impurities will not exceed 1%.

In order to achieve full acceptance coverage for the Cherenkov photons emitted by pions and muons, the total surface of the mirrors will have a diameter of about 3 m. To avoid absorption of reflected light on the beam pipe, the mirrors are divided into two spherical surfaces: one with the centre of curvature to the left and one to the right of the beam pipe. Since the total reflective surface exceeds  $6 \text{ m}^2$ , a matrix of 20 mirrors, 18 hexagonal (each inscribed inside a 70 cm diameter circle) and 2 semi-hexagonal, will be used. The mirrors are made of 25 mm thick glass substrate coated with aluminium and covered with a thin dielectric film in order to protect the surface and to improve the reflectivity. Each mirror will be individually supported and adjusted for alignment. A carbon fiber honeycomb structure will hold the mirrors, and piezo-actuators will be used for the movement.

On the opposite side of the mirror location at the upstream end, two flanges, each about 1 m far to the left and to the right of the beam pipe axis, will house the PM's that are regularly distributed to instrument these two regions. The PM's are separated from the neon by means of 1 mm thick quartz windows, and Winston's cones [8] are used to enhance the ratio between sensitive and instrumented areas. The Hamamatsu R7400-U03 metal package PM has been chosen as the light detector because of its speed (280 ps FWHM transit time jitter), small dimensions (16 mm wide with an active diameter of 8 mm) and relative cheapness. Thanks to the UV-glass window and bi-alkali cathode, the PM has good response up to the near ultraviolet with a peak quantum efficiency of about 20% at 420 nm. The PM will be operated at  $\sim 900 \text{ V}$  negative voltage with a gain of about  $1.5 \times 10^6$ . The high voltage system will consist of CAEN SY1527 and SY2527 crates equipped with A1733N boards. The PM signal is sent to a custom-made current amplifier with differential output. The amplifiers feed NINO chips [9] used as discriminators operating in time-over-threshold mode, providing a fast LVDS signal.

The RICH detector readout is a compact, high-performance TDC-based integrated read-out and trigger system. The TEL62 mother board [10], which is partly based on existing hardware developed for LHC experiments (TELL1 [11]), can house up to four custom daughter-cards, each of them served by a FPGA and a large amount of dynamic memory. A TDC daughter-card was developed for NA62, based on CERN HPTDC chips [12], working in 100 ps LSB resolution mode. A single daughter card houses 128 channels for a total of 512 channels per board. The trigger primitives will be constructed in parallel with the readout on the same mother board.

## TEST BEAM RESULTS

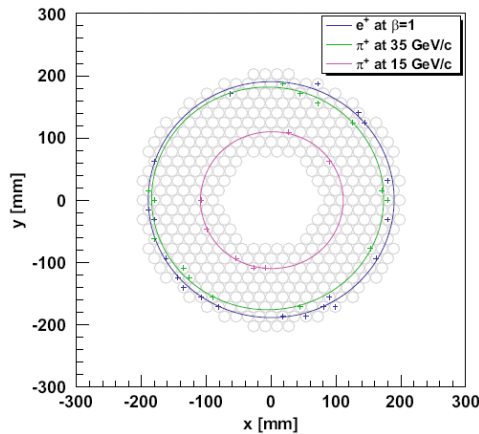
A RICH prototype was built and tested at CERN. A stainless steel vessel, 17 m long and 60 cm wide (divided in 5 sections) and vacuum resistant, was installed along the K12 beam line in the SPS North Area. A single spherical mirror, 50 cm in diameter and 25 mm thick, with a focal length of 17 m was used. The mirror was placed at the downstream end of the vessel, mounted on a support structure that could be moved by means of two remotely controlled step motors. At the upstream end, a stainless steel flange was placed to house the PM's that are arranged in a hexagonal lattice (honeycomb). Each PM was separated from neon by a 1 mm thick quartz

window; a Winston cone covered with a thin mylar foil was used to convey the light to each PM, as it is foreseen for the final detector.

A first test was performed in October 2007. The RICH prototype was exposed to a 200 GeV/c momentum negative beam composed mainly of pions. The detector was equipped with a limited number of PM's (96) placed in the region where the 200 GeV/c pion Cherenkov ring was expected. This test was mainly devoted to the assessment of the final choice of the PM and to the measurement of the time resolution and Cherenkov angle resolution. The U03 and U06 types of the Hamamatsu R7400 PM were tested. Type U03 was chosen because the U06 type was more expensive, had worse time resolution and did not provide a significantly higher number of photoelectrons. An average single PM time resolution of 310 ps was found, while the RMS of the average event time was measured to be about 65 ps. The pion Cherenkov angle resolution turned out to be better than 60  $\mu$ rad and the average number of PMs that fired per event was found to be 17. The prototype construction and the results from this test are described in detail in [13].

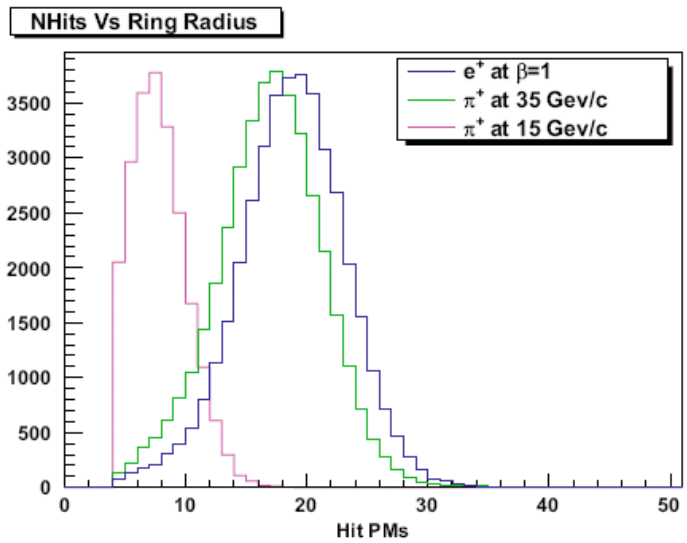
The RICH prototype was tested again at CERN in May-June 2009. The main improvements with respect to the previous test were a larger number of PMs, a new read-out electronics based on TEL62 and TDC boards, and a cooling system. The upstream flange of the vessel was redesigned to accommodate 414 PMs, in order to cover the whole acceptance for Cherenkov light produced by positive pions with momentum  $\geq 15$  GeV/c passing through the detector along its axis and to house a cooling system to be used in the final detector. Positive hadron beams produced by the SPS primary 400 GeV/c protons were used at different momenta in the 10 GeV/c to 75 GeV/c range in order to measure the  $\pi$ - $\mu$  separation, to check the detector performance and to validate the design of the final read-out electronics. The beam was composed mainly of pions with a small quantity of protons, a few percent of kaons and a variable fraction of positrons. The prototype performances were tested under different conditions: beam momenta, mirror orientation, rates, TEL62 firmware versions and gas contamination (adding air and CO<sub>2</sub> to neon). The measurements were repeated with a new mirror that is similar to the final ones.

Figure 2 shows a typical event with well separated reconstructed ring images for, in order of decreasing radii, positrons ( $\beta=1$ ), pions at 35 GeV/c and pions at 15 GeV/c.



**FIGURE 2.** Reconstructed ring images for, in order of decreasing radii, positrons ( $\beta=1$ ), pions at 35 GeV/c and pions at 15 GeV/c.

The average number of PM hits in a single ring, shown in Fig. 3, is about 20 for positrons (rightmost histogram), 17 for pions at 35 GeV/c (middle histogram) and 8 for pions at 15 GeV/c (leftmost histogram).



**FIGURE 3.** Distribution of the number of hit PMs in a single ring; the cut at 4 is due to the software trigger algorithm.

The number of hit PMs per ring as a function of the momentum is shown in Fig. 4. The time resolution, shown in Fig. 5a, is defined as the average root mean square of the distribution of the selected hit times with respect to the average hit time: a value below 100 ps has been measured over the momentum range of interest.

The Cherenkov angle resolution as a function of the pion momentum is presented in Fig. 5b. The standard deviation is estimated by a Gaussian fit to the radius distribution excluding tails; the resolution decreases to a constant value of about 70  $\mu\text{rad}$  for  $\beta=1$  particles.

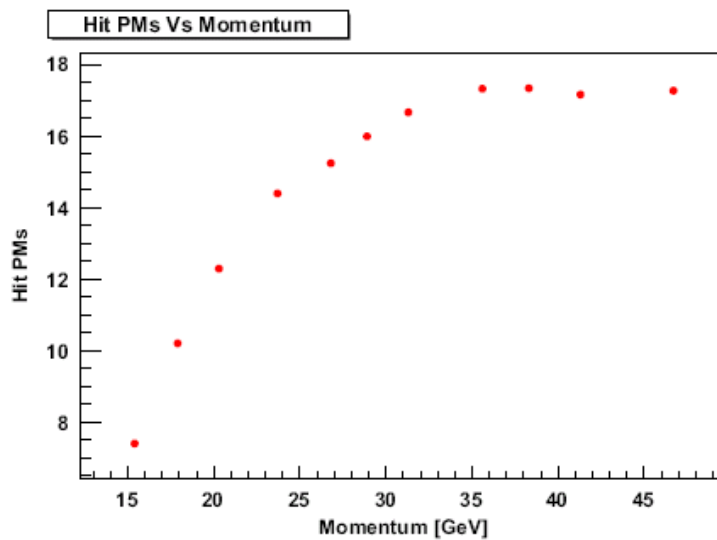


**FIGURE 4.** Average number of hit PMs per ring as a function of momentum.

The small rising trend in the high momentum region is associated with variations in light acceptance as a result of geometrical effects due to the honeycomb structure. Both time and Cherenkov angle resolution are strongly correlated to the number of hit PMs per ring, hence to the number of Cherenkov photons and to the collection and the detection efficiencies.

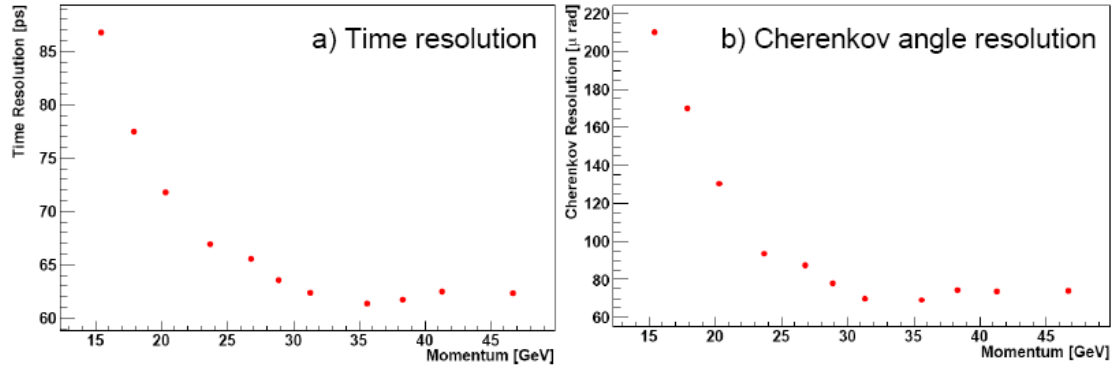
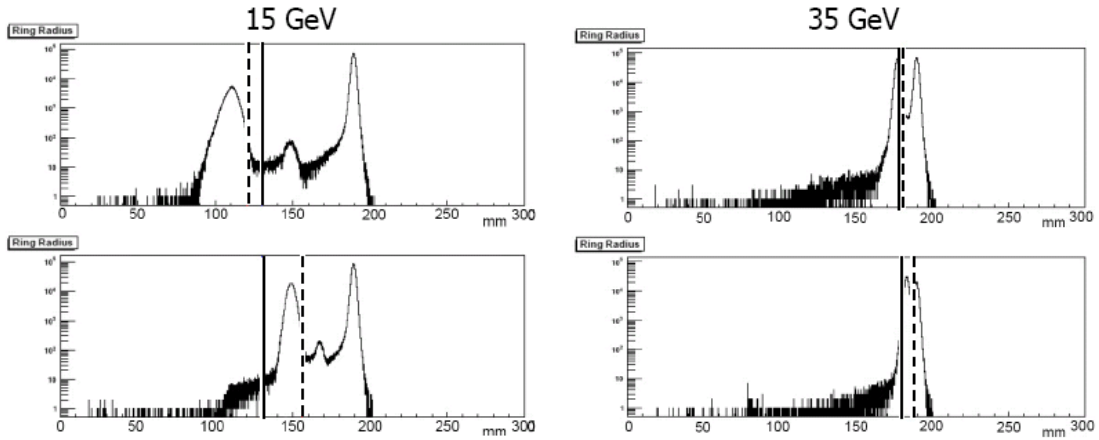


FIGURE 5. (a) Time resolution and (b) Cherenkov angle resolution as a function of the momentum.

The  $\pi$ - $\mu$  separation in the momentum range 15-35 GeV/c was measured using only pions since the muon content in the beam was negligible. The following method was used: the fitted Cherenkov ring radius for pions at a given momentum was compared with the radius of pions at higher momentum and with the same  $\beta$  that a muon would have at the original momentum. For example, the ring radius of pions at 15.2 GeV has been compared with the ring radius of pions at 20.0 GeV (fake muons). The  $\pi$ - $\mu$  separation was parameterized by the probability of misidentifying a  $\pi$  as a  $\mu$ . In each momentum bin, a signal region ( $\pi$ ) was defined and the fraction of “ $\mu$ ” in that region was evaluated. The procedure to calculate the misidentification probability is the following: a Gaussian fit, excluding tails, to both peaks was used to extract their average values and their widths; the normalization for  $\mu$ 's is taken as the number of events within 3 standard deviations from its average, while a cut half-way between the two peaks is used to separate signal and background regions. Since the  $\pi$ - $\mu$  separation has been calculated using two data samples at two different momenta, the systematic effect due to its knowledge can be estimated by comparing the results obtained using two different variables. As an example of the technique illustrated, Fig. 6 shows the fitted Cherenkov ring radius distribution used for the  $\pi$ - $\mu$  separation measurement at two different momentum bins: 15 GeV/c (left) and 35 GeV/c (right). The top part of the figures refers to the pion samples: peaks correspond, from left to right, to pions, real muons due to pion decays in flight, and positrons at 15 GeV/c (left) and at 35 GeV/c (right) momenta. The bottom parts of the figures represent the muon samples, simulated with pions at higher momenta with the same  $\beta$  of muons at 15 GeV/c (left) and 35 GeV/c (right), namely 20 and 46.3 GeV, respectively. After defining the pion signal as all the events within  $+3\sigma$  from the peak of the distribution (dotted lines in Fig. 6), a cut is set at half way between the  $\pi$  and the  $\mu$  signal peaks (solid lines in Fig. 6) in order to calculate the pion loss and the muon contamination.



**FIGURE 6.** Reconstructed ring radius distributions used for the measurement of  $\pi$ - $\mu$  separation at 15 GeV/c (left) and 35 GeV/c (right). See text for details.

The clear  $\pi$ - $\mu$  separation is more evident at lower momentum due to the increase of the distance between muon and pion ring radii. The quantitative evaluation of the separation is based on the integral of many measurements done at different momentum and experimental conditions, i.e. mirror orientation, analysis cut, etc. Figure 7 shows the muon misidentification probability as a function of the particle momentum, measured for four different positions of the mirror with respect to the beam line in order to take into account possible displacements of the ring center. Figure 8 represents the same measurement repeated with different event selections and ring reconstruction methods: the upper and the lower limits are the  $3\sigma$  constraint on the position of the fitted ring center. The overall integral of the measurements gives a muon misidentification probability of  $< 0.7\%$ , measured in many different conditions and very close to the requested  $0.5\%$ . Further details on the results of the test of the RICH-400 prototype can be found in [14].

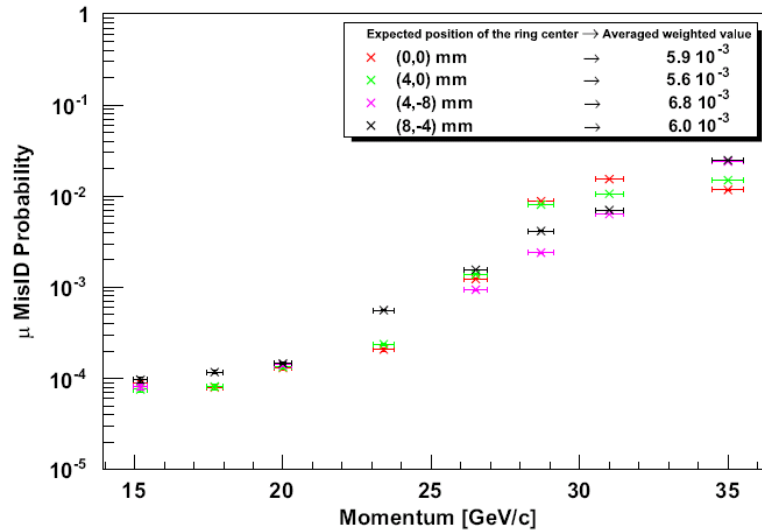


**FIGURE 7.** Muon misidentification probability as a function of momentum for four different alignment positions of the mirror.

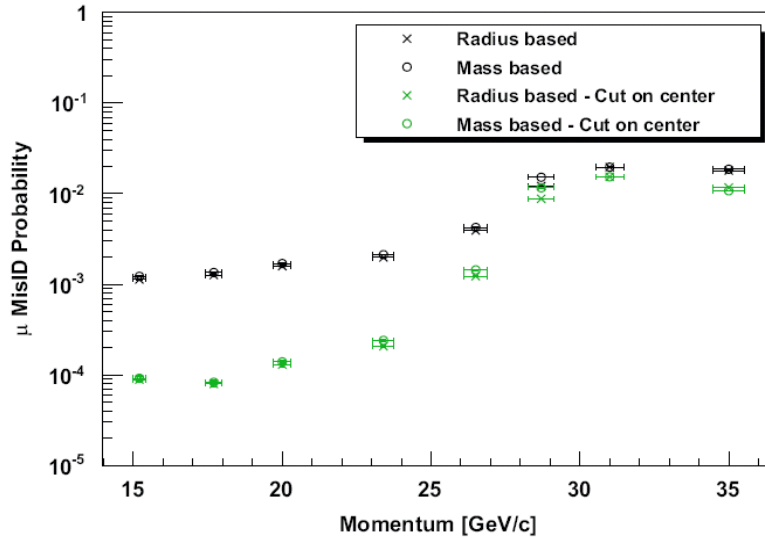


**FIGURE 8.** Muon misidentification probability as a function of momentum for different cuts and ring reconstruction methods.

In conclusion, the design parameters of the NA62 RICH detector have been validated by the results of the test beams of a full longitudinal scale prototype, performed at CERN in 2007 and 2009. The project matches the requirements expected for the NA62 experimental program; the final detector is in construction and will be ready for the data taking foreseen in 2012-2013.

## ACKNOWLEDGMENTS

This work was partially supported by Fondazione Cassa di Risparmio di Perugia, Progetti Ricerca di Base “La fisica del sapore nell’era di LHC”. It is a pleasure to thank the Organizing Committee for the very interesting conference and stimulating discussions and also for the nice time I had in Crete.

## REFERENCES

1. G. Anelli et al., *CERN-SPSC-2005-013*, *CERN-SPSC-P-326* (2005).
2. J. Brod and M. Gorbahn, *Phys. Rev. D* **78**, 034006 (2008).
3. A.V. Artamonov et al., *Phys. Rev. D* **79**, 092004 (2009).
4. G. Isidori et al., *JHEP* 0608 064 (2006), hep-ph 0604074.
5. M. Blanke et al., *JHEP* 0701 066 (2007), hep-ph 0610298.
6. J. Seguinot and T. Ypsilantis, *Nucl. Instr. and Meth. A* **142**, 377 (1977).
7. G. Anelli, et al., *NA62/P326 Status Report*, *CERN-SPSC-2007-035*, (2007).
8. R. Winston, *J. Opt. Soc. Am.* **60**, 245-247 (1970).
9. F. Anghinolfi et al., *Nucl. Instr. and Meth. A* **533**, 183-187 (2004).
10. C. Avanzini et al., *Nucl. Instr. and Meth. A* **623**, 543-545 (2010).
11. G. Haefeli et al., *Nucl. Instr. and Meth. A* **560**, 494-502 (2006).
12. M. Mota and J. Christiansen *JSSC* vol **34**(10), 1360-1366 (1999).
13. G. Anzivino et al., *Nucl. Instr. and Meth. A* **593**, 314-318 (2008).
14. B. Angelucci et al., *Nucl. Instr. and Meth. A* **621**, 205-211 (2010).